Levels of soluble apolipoprotein E/amyloid-β complex are reduced and oligomeric Aβ increased with *APOE4* and Alzheimer disease in a transgenic mouse model and human samples

Leon M Tai[1], Tina Bilousova[2], Lisa Jungbauer[1,a], Stephen K Roeske[1], Katherine L. Youmans[1b], Chunjiang Yu[1], Wayne W. Poon[3], Lindsey B. Cornwell[3], Carol A. Miller[4], Harry V. Vinters[5], Linda J. Van Eldik[6,7], David W. Fardo[6,8], Steve Estus[6,9], Guojun Bu[10], Karen Hoppens Gylys[2], and Mary Jo LaDu[1*]

From the [1]Department of Anatomy and Cell Biology, University of Illinois, Chicago, IL, USA, the [2]UCLA School of Nursing and Mary S. Easton Center for Alzheimer's Research, Los Angeles, CA, USA, the [3]Institute for Memory Impairments and Neurological Disorders, UC Irvine, Irvine, CA, USA, the [4]Departments of Pathology, Neurology, and Program in Neuroscience, Keck USC School of Medicine, Los Angeles, CA, USA, the [5]Department of Pathology and Laboratory Medicine, UCLA School of Medicine, Los Angeles, USA, the [6]Sanders-Brown Center on Aging, University of Kentucky, Lexington, KY, the [7]Department of Anatomy and Neurobiology, University of Kentucky, Lexington, KY, the [8]Department of Biostatistics, University of Kentucky, Lexington, KY, the [9]Department of Physiology, University of Kentucky, Lexington, KY, and the [10]Department of Neuroscience, Mayo Clinic, Jacksonville, FL, Present address [a]Medtronic, Inc., 7000 Central Ave NE, RCE470, Minneapolis, MN 55432,[b] Department of Pharmacology, Boston University, Boston, MA 02215.

Running title: *APOE-genotype* effects on soluble apoE/Aβ complex levels

*To whom all correspondence should be addressed: Mary Jo LaDu, University of Illinois at Chicago, Department of Anatomy and Cell Biology, 808 S.Wood St., M/C 512, Chicago, IL 60612, USA. Phone: 312-355-4795; Fax: 312-413-0354; Email: mladu@uic.edu

Keywords: apolipoprotein E; amyloid-β; apoE/Aβ complex; oligomeric Aβ, ELISA; Alzheimer's disease; synaptosomes; CSF; biomarkers

Background: An ELISA was developed to determine the role of apoE/Aβ complex on soluble Aβ accumulation.

Results: In AD transgenic mouse brain and human synaptosomes and CSF, levels of soluble apoE/Aβ are lower and oligomeric Aβ higher with *APOE4* and AD.

Conclusion: Isoform-specific apoE/Aβ levels modulate soluble oligomeric Aβ levels.

Significance: ApoE/Aβ and oligomeric Aβ represent a mechanistic approach to AD biomarkers.

ABSTRACT

Human apolipoprotein E (apoE) isoforms may differentially modulate amyloid-beta (Aβ) levels. Evidence suggests physical interactions between apoE and Aβ are partially responsible for these functional effects. However, apoE/Aβ complex is not a single, static structure; rather, it is defined by detection methods. Thus, literature results are inconsistent and difficult to interpret. An ELISA was developed to measure soluble apoE/Aβ complex in a single, quantitative method, and used to address the hypothesis that reduced levels of soluble apoE/Aβ complex and an increase in soluble Aβ, specifically oligomeric Aβ (oAβ) are associated with *APOE4* and AD. In a previous study, soluble Aβ42 and oAβ levels were greater with *APOE4* compared with *APOE2*/*APOE3* in hippocampal homogenates from EFAD transgenic mice (expressing 5 familial AD mutations and human apoE isoforms). In the current study, soluble apoE/Aβ levels were lower in E4FAD mice compared with E2FAD and E3FAD, evidence that apoE/Aβ levels isoform-specifically modulate soluble oAβ clearance. Similar results were observed in soluble preparations of human cortical synaptosomes; apoE/Aβ levels were lower in AD patients compared to controls, and lower with *APOE4* in the AD cohort. In human CSF, apoE/Aβ levels were also lower in AD patients and with *APOE4* in the AD cohort. Importantly, although total Aβ42 levels decreased in AD patients compared to controls, oAβ levels

increased and were greater with *APOE4* in the AD cohort. Overall, apoE isoform-specific formation of soluble apoE/Aβ complex modulates oAβ levels, suggesting a basis for *APOE4*-induced AD risk and a mechanistic approach to AD biomarkers.

INTRODUCTION

APOE4 is the primary genetic risk factor for Alzheimer disease (AD), while *APOE2* reduces risk compared to *APOE3*. Although the mechanism(s) by which apolipoprotein E (apoE) and amyloid-β peptide (Aβ) affect the pathogenesis of AD remains unclear (for review (1,2)), apoE isoform-specific physical interactions with Aβ (apoE/Aβ complex) may modulate the levels of Aβ. These interactions appear to consist of two types, which may or may not be "on pathway" to amyloid deposition: apoE isoform-specific effects on plaque development and apoE isoform-specific effects on the levels of soluble, oligomeric aggregates of Aβ (oAβ). For this study, an apoE/Aβ complex ELISA was developed to determine the effect of *APOE* genotype on the levels of soluble apoE/Aβ complex and Aβ.

The amyloid hypothesis posits that deposition of extracellular amyloid is central for producing the neurodegenerative processes characteristic of AD (3). In the landmark 1992 paper, Wisniewski and Frangione proposed that apoE was a "pathological chaperone", based on the co-localization of apoE with Aβ in amyloid plaques as detected via immunohistochemistry (IHC) (4). Thus, apoE was thought to facilitate the process of Aβ deposition as amyloid. Biochemical analyses validate IHC measures, as the levels of apoE and Aβ are equivalent in the insoluble extraction fraction from brains of transgenic mice expressing familial AD (FAD) mutations (FAD-Tg), specifically the 5xFAD-Tg mice (5). The association of *APOE4* with AD risk was first described in 1993 (6,7), leading to research efforts focused on the effects of *APOE* genotype on plaque burden and the structural relationship between apoE and amyloid. IHC analysis demonstrates that plaque deposition is greater with *APOE4* compared to *APOE3* in AD and non-demented controls (8,9), and that a higher proportion of Aβ within a plaque is associated with apoE4 than with apoE3 (10). Biochemical analysis confirms that the levels of apoE and Aβ are also higher with *APOE4* compared to *APOE3* in the insoluble extraction fraction from brains of FAD-Tg mice (11). Thus, *APOE4* not only facilitates amyloid deposition but also forms a greater amount and/or more stable form of apoE4/amyloid than apoE3/amyloid.

The amyloid hypothesis has been revised, as plaque burden does not correlate with the dementia that is characteristic of AD (12,13). However, soluble Aβ and oAβ do correlate with cognitive decline and disease severity in humans (14). oAβ is also detected in FAD-Tg-mice and is associated with memory decline (for review (14)). Thus, the structure-function relationship of soluble Aβ and oAβ is an area of intense research. However, unlike amyloid, which refers to a specific parallel β-sheet structure, oAβ refers to a number of assemblies defined by a variety of detection methods (14). This makes interpretation and comparison of results problematic, particularly with *in vivo* data. We recently developed an oAβ ELISA and demonstrated that in EFAD-Tg mice, soluble Aβ42 and oAβ are greater in E4FAD mice, compared to E2FAD and E3FAD (15). Aβ clearance also appears to be decreased with *APOE4* (16), suggesting that soluble apoE/Aβ complex may modulate soluble Aβ and oAβ levels.

Research efforts to determine apoE/Aβ complex levels, particularly soluble complex levels, have been hindered by a lack of quantitative detection methods. A variety of techniques have produced results that can be inconsistent and difficult to interpret (7,17-27). Even the initial biochemical characterization of the molecular interactions between apoE and Aβ were problematic, primarily because of two parameters. The first variable was the lipidation state of apoE. Using purified protein, apoE4 bound Aβ with a higher affinity than apoE3 (28,29). However, this result is reversed using physiologically relevant, lipidated apoE; levels of apoE3/Aβ complex are significantly greater than apoE4/Aβ complex (21,28,29). Second, the definition of an apoE/Aβ complex is primarily operational, with assay stringency the primary variable (7,17-27,30). For example, apoE3/Aβ levels are greater than apoE4/Aβ as determined by Western analysis of

SDS-PAGE (21), but by non-denaturing gel electrophoresis levels of apoE3/Aβ complex are comparable to apoE4/Aβ (31). Although these data are consistent with a SDS-stable apoE3/Aβ complex (reviewed in (32)), and an apoE4/Aβ complex that is disrupted by SDS, the total amount of apoE/Aβ complex cannot be quantified by Western analysis of SDS-PAGE. The first goal of this study was to define biochemically-generated apoE/Aβ complex in the context of a single quantitative and potentially high throughput method that would also define both total and detergent (SDS)-stable apoE/Aβ complex, providing a platform for comparison among apoE isoforms and across methods. Thus, a new apoE/Aβ ELISA was developed and optimized biochemically. *In vitro*, total complex levels were equivalent among the apoE isoforms, although apoE3/Aβ complex was more SDS-stable than apoE4/Aβ complex but was less SDS-stable than apoE2/Aβ. These results are consistent with previous results utilizing several methods that suggest the levels of apoE3/Aβ and apoE4/Aβ complex are comparable in the absence of SDS but that SDS-stable apoE3/Aβ complex levels are greater than apoE4/Aβ (18,21,22,27).

In contrast to biochemical analysis, the number of *in vivo* reports on soluble apoE/Aβ complex is limited. ApoE/Aβ complex has been detected in the soluble fraction of human brain (33) and in human cerebrospinal fluid (CSF) (30,34), although the data were primarily produced using Western analysis of SDS-PAGE. By IHC, apoE also co-localizes with Aβ at the synapse (35) and insoluble apoE/Aβ complexes appear to form preferentially with apoE4 compared to apoE3 (36). However, the effect of *APOE* genotype on soluble synaptic apoE/Aβ complex levels remains unclear (37-40). Thus, the new apoE/Aβ ELISA was used *in vivo* to determine the levels of soluble apoE/Aβ complex and the effect of *APOE* genotype. In EFAD transgenic mice, previous data demonstrated that with *APOE4,* soluble Aβ42 and oAβ levels were greater (15) and in data presented herein, soluble apoE4/Aβ complex levels were lower and less stable compared to apoE3/Aβ and apoE2/Aβ levels. In human synaptosome preparations and CSF, apoE/Aβ levels were lower in AD compared to controls, and with *APOE4* compared to *APOE3* in the AD cohort. Importantly, in human CSF, although total Aβ42 levels decreased in AD patients compared to controls, oAβ levels increased and were greater with *APOE4* in the AD cohort. Taken together, the low levels of soluble apoE4/Aβ complex and high levels of soluble oAβ suggest an impaired clearance mechanism for soluble forms of Aβ and a potential basis for *APOE4*-induced AD risk, as well as a mechanistic approach to CSF biomarkers for AD.

EXPERIMENTAL PROCEDURES

Materials

High-bind (Maxisorp™) and low-bind plates (Microwell™) were purchased from NUNC, Rochester, NY). Anti (α)-Aβ antibodies used were: 6E10 (Covance Labs, Madison, WI), 4G8 (Senetek, Maryland Height, MD) and MOAB-2 (41) (LaDu laboratory and available from: Abcam, Cambridge, MA; Biosensis, Temecula, CA; Millipore, Bilerica, MA; Novus, Littleton, CO; and Cayman, Ann Arbor MI). Goat α-apoE antibodies were from Calbiochem (Cal, Gibbstown, NJ), Meridian (Mer, Memphis, TN), and Milipore (Mil, Bilerica, MA). Recombinant apoE3 was from BioVision (Milpitas, CA) and synthetic Aβ peptides were from California Peptide (Napa, CA).

HEK-apoE

ApoE from HEK-293 cells stably transfected with human cDNA encoding apoE2, apoE3 or apoE4 was prepared as previously described (21,42,43). Briefly, serum-free conditioned media was concentrated ~50-fold (Centriprep, Amicon, Inc.) and fractionated by size exclusion chromatography (SEC). The resulting fractions containing apoE particles were pooled and the concentration of apoE quantified.

Amyloid-beta (Aβ) peptide

Aβ peptides were prepared as previously described (44-46). HFIP treated Aβ was dissolved in DMSO to 5 mM, and then to 100 μM in phenol red-free F12 media (BioSource, Camarillio, CA) for unaggregated and oAβ or 10 mM HCl for fibrillar Aβ. Unaggregated Aβ was freshly prepared just prior to use, oAβ42 preparations

were aged for 24 h at 4°C and fibrillar Aβ42 preparations for 24 h at 37°C.

ApoE/Aβ complex standard development and biochemical characterization

ApoE/Aβ complex formation - HEK-apoE or recombinant apoE and Aβ were incubated at the indicated concentrations for 2 h at room temperature (pH 7.4) with SDS (Sigma-Aldrich) or vehicle at the indicated concentrations. The pH profile for apoE/Aβ complex levels was conducted as described (21).

ELISA Curve fitting - In the absence of SDS: The EC50 for Aβ and apoE was calculated using the 4-parameter logistic equation:

ApoE/Aβ complex levels = Bottom + (Top-Bottom)/(1+10^((LogEC50-X)*HillSlope))

Top and bottom represents the apoE/Aβ complex levels at the plateaus. EC50 is the concentration of Aβ or apoE that produces 50% maximal response. X is the concentration of the variable i.e. Aβ or apoE.

In the presence of SDS: The IC50 for SDS was calculated according to the following equation:

ApoE/Aβ complex levels (% of control) = 100/(1+10^(X-LogIC50))

IC50 is the effective concentration of SDS that produces 50% response. X corresponds to the concentration of SDS.

Analysis was conducted for each individual experiment, and data were analyzed using one-way analysis of variance (ANOVA) followed by Tukey's post-hoc analysis GraphPad Prism version 5 for Macintosh was used for all curve fitting analysis.

ApoE/Aβ complex ELISA

Biochemical ELISA development - In order to accurately quantify total and SDS-stable levels of apoE/Aβ complex, a specific ELISA was developed. ApoE/Aβ complex formed between HEK-apoE and unaggregated Aβ42 was utilized for ELISA development. To minimize non-specific binding of apoE and Aβ, and maximize apoE/Aβ complex detection, a number of antibody combinations were screened as capture or detection antibodies on NUNC Maxisorp™ (high-bind) or Microwell™ (low bind) plates (Supplemental Figure 1). Results demonstrated that: 1) Non-specific binding of Aβ to high- and low-bind plates precludes the use of α-Aβ antibodies for detection: 2) Non-specific binding of HEK-apoE prevents the use of high-bind plates (Supplemental Figure 1A); 3) ApoE/Aβ complex, but not apoE or Aβ, is detected on low-bind plates using α-apoE capture and α-Aβ detection antibodies (Supplemental Figure 1B) and; 4) α-Aβ (MOAB-2) capture and α-apoE (Cal) detection antibodies produces the highest signal/background ratio compared to other antibodies tested (Supplemental Figures 1C and 1D). Thus, the optimal reagents/conditions for specific HEK-apoE/Aβ complex detection by ELISA were: low-bind 96 well plates with α-Aβ (MOAB-2) capture and α-apoE (Cal) detection antibodies.

ApoE/Aβ ELISA - Protocol 1: Low-bind plates were coated with MOAB-2 at 6.25 μg/ml in carbonate coating buffer overnight at 4°C. Plates were washed (3x in PBS), blocked (4% BSA, 1.5h, 37°C), washed again (3x in PBS) and incubated with samples overnight. The plates were then washed (3x in PBS), incubated with a 200-fold dilution of α-apoE (Cal) (1.5h, 37°C), washed, and incubated with HRP-conjugated antibodies (1.5 h, RT, 1:5000 dilution, Jackson Immuno-Research, West Grove, PA). Following a final wash step (3x in PBS), TMB Superslow (Sigma-Aldrich) substrate was added, and absorbance measured at A620. *Protocol 2:* All steps are identical to *protocol 1*, with the exception that high-bind plates were utilized (See CSF results description).

Soluble apoE/Aβ complex detection in EFAD mice

EFAD transgenic mice - Experiments follow the UIC Institutional Animal Care and Use Committee protocols. EFAD mice (15) are the result of crossing 5xFAD mice, which co-express 5 Familial AD mutations (APP K670N/M671L + I716V + V717I and PS1 M146L + L286V) under the control of the Thy-1 promoter with apoE-targeted replacement mice. Details on the production, breeding, genotyping, and genetic background of these mice are described in (15) .

Tissue preparation - Brain tissue isolation and serial protein extraction were conducted as previously described (5,15). Briefly, 6-month old

male EFAD mice were anesthetized with sodium pentobarbital (50 mg/kg), transcardially perfused (PBS plus protease inhibitors (Calbiochem, set 3)), and brains were removed and dissected at the midline. Right hemi-brains were dissected on ice into cortex (CX), hippocampus (H) and cerebellum (CB), immediately snap frozen in liquid nitrogen, and stored at -80°C until use. The dissected tissue was homogenized in 15 volumes (w/v) of TBS, samples were centrifuged (100,000xg, 1 h at 4°C) and the TBS (soluble) fraction was aliquoted prior to freezing in liquid nitrogen and storage at -80°C.

ApoE/Aβ complex - The apoE/Aβ levels were measured using a 4-fold sample dilution of the TBS extraction fraction from the hippocampus of EFAD mice according to apoE/Aβ ELISA *protocol 1*. The standard curve used a fixed HEK-apoE concentration of 140 nM (apoE concentration in the TBS extraction of EFAD mice at 6 months for all *APOE* genotypes) and varied Aβ concentrations. Data were normalized to protein concentration in each sample.

ApoE/Aβ detection in human synaptosomes

Brain samples of parietal cortex (A7, A39, A40) were obtained at autopsy for cases followed by the Alzheimer's disease research centers at UCLA, UCI and USC (Supplementary Table 1); the last clinical diagnosis and full neuropathological report and diagnosis were available for all cases. Control samples included normal cases and pathological controls. Immediately on receipt, samples (~0.3-5 g) were minced in 0.32 M sucrose with protease inhibitors (2 mM EDTA, 2 mM EGTA, 0.2 mM PMSF, 1 mM Na pyrophosphate, 5 mM NaF, 10 mM Tris), then stored at -70°C until homogenization. The P-2 (crude synaptosome; synaptosome-enriched fraction) was prepared as previously described (42); briefly, tissue was homogenized in ice cold buffer (0.32M sucrose, 10 mM TRIS pH 7.5, plus protease inhibitors: pepstatin (4 mg/ml), aprotinin (5 mg/ml), trypsin inhibitor (20 mg/ml), EDTA (2mM), EGTA (2 mM), PMSF (0.2 mM), Leupeptin (4 mg/ml). The homogenate was first centrifuged at 1000 *g* for 10 min; the resulting supernatant was centrifuged at 10,000 *g* for 20 min to obtain the crude synaptosomal pellet. Aliquots of P-2 are routinely cryopreserved in 0.32 M sucrose and banked at -70°C until the day of the experiment. On the day of the experiment, cryopreserved human P-2 aliquots were defrosted at 37°C, resuspended in PBS with protease inhibitors, sonicated and centrifuged for 4 min at 6,000 rpm. Supernatant was collected and total protein concentration was defined using BCA protein assay (Pierce). ApoE/Aβ complex levels were measured using a 5-fold sample dilution according to apoE/Aβ ELISA *protocol 1*. The standard curve used a fixed HEK-apoE concentration of 14 nM (apoE concentration in the synaptosomes), and varied Aβ concentrations. Human data were normalized according to total protein concentration in each sample.

ELISA analysis of human CSF

CSF samples were obtained on autopsy at the Alzheimer's disease center at the University of Kentucky (Supplementary Table 2). Diagnoses of AD and non-AD were performed at a consensus conference of the AD Center Neuropathology and Clinical Cores and were based upon evaluation of both cognitive status, i.e., Clinical Dementia rating and Mini-Mental State Examination (MMSE) scores, as well as neuropathology, i.e., Braak stages which rate the extent of neurofibrillary pathology into the neocortex and NIAReagan Institute (NIA-RI) neuropathology classification, which includes counts of both neuritic senile plaques and neurofibrillary tangles and provides a likelihood staging of AD neuropathological diagnosis (47,48). For ELISA analysis: Aβ42, total tau (T-tau) and phosphorylated tau 181 (P-tau-181) levels were measured using Innotest® ELISA kits (Innogenetics Gent, Belgium) according to the manufacturers protocol; apoE levels were measured using α-apoE (Mil) as capture and α-apoE (Mer) as detection as described (11). oAβ levels were measured using MOAB-2 capture (5) and biotinylated MOAB-2 as detection antibody as described in (15). ApoE/Aβ complex levels were measured using a 2-fold sample dilution according to apoE/Aβ ELISA *protocol 2*, with a standard curve of 5 μg/ml recombinant apoE (reported CSF apoE concentration) and varied Aβ concentrations.

Statistical analysis

Data were analysed by one-way analysis of variance (ANOVA) followed by Tukey's post-hoc analysis, (Figures 2A, 2B, 3, 4 and 5) or by two-way ANOVA followed by Bonferroni post hoc analysis (Figure 2C). Correlation analysis was conducted using Spearman's correlation (Figure 5E and 5F). All data were analysed using GraphPad Prism version 5 for Macintosh and $p < 0.05$ was considered significant. Receiver operating characteristic (ROC) curves (Figure 6) were constructed for each marker using the pROC package in R (49,50). Areas under the curves were compared by the method of DeLong and co-workers (51).

RESULTS

Biochemical development of apoE/Aβ complex ELISA

Initially, biochemical analysis using HEK-apoE and synthetic Aβ preparations (45) (Figure 1) was conducted to; 1) validate the apoE/Aβ complex ELISA, and; 2) determine the effect of apoE isoform on soluble apoE/Aβ complex levels and stability.

Total apoE/Aβ complex levels are not affected by apoE isoform.

Total complex levels were measured in samples containing a fixed apoE concentration (30 nM), and a varied concentration of unaggregated Aβ42, (0.15-150 nM) (Figure 1A) or using varied apoE concentration (0-1500 nM) and a fixed Aβ concentration (3 nM) (Figure 1B). Overall, apoE/Aβ complex levels were saturable and dependent on apoE and Aβ concentrations but not apoE isoform. Indeed, when these data were analysed using a 4-parameter logistic equation, which is appropriate for analysing ELISA saturation curves (52), there were no differences between the calculated EC50s among the apoE isoforms (~ 3 nM for Aβ in Figure 3A and ~ 30 nM for apoE in Figure 1B). Total apoE/Aβ complex levels were also equivalent for apoE2, apoE3 and apoE4 with unaggregated Aβ40, oAβ42 and fibrillar Aβ42 (data not shown). Thus, apoE isoform does not determine total apoE/Aβ complex levels biochemically.

ApoE2/Aβ and apoE3/Aβ complex exhibits greater stability than apoE4/Aβ complex

As apoE isoform did not affect total complex levels when assessed by ELISA, SDS was added to samples as a measure of stability (Figure 1C). ApoE and Aβ were incubated for 2 h at concentrations that correspond to the EC50 values identified for total apoE/Aβ complex levels, specifically 3 nM Aβ42 and 30 nM apoE, and then SDS was added over a range of concentrations (up to 2%). Complex stability from highest to lowest was: apoE2/Aβ > apoE3/Aβ > apoE4/Aβ. This was evident as the SDS IC50 was 1.5-fold higher for apoE2/Aβ complex and 3-fold lower for the apoE4/Aβ complex compared to the apoE3/Aβ complex. In addition to SDS, the apoE4/Aβ complex was less stable at mildly acidic pH (5) than apoE2/Aβ and apoE3/Aβ complex (Figure 1D). Therefore, apoE/Aβ complex levels are not determined by apoE isoform; however, the apoE4/Aβ complex is less stable and the apoE2/Aβ more stable than the apoE3/Aβ complex.

Soluble apoE/Aβ complex levels in EFAD mice

In order to determine the effect of *APOE* genotype on soluble apoE/Aβ complex levels, the tractable EFAD mouse model was utilized. For this study, apoE/Aβ complex levels were measured in the soluble hippocampal homogenates from EFAD mice at 6 months (Figure 2), an age where soluble oAβ levels are greater in E4FAD (*APOE4*) compared with E2FAD (*APOE2*) and E3FAD (*APOE3*) mice (15).

ApoE/Aβ complex ELISA optimization in EFAD mice

Initially, soluble apoE/Aβ complex detection by ELISA was validated using E3FAD mice at 6-months (Figure 2A). For a quantitative standard to enable cross plate comparisons, complex formed between HEK-apoE3 at a fixed concentration of 140 nM, which corresponds to soluble apoE levels in EFAD mice at 6 months, and a varied concentration of unaggregated Aβ42 was utilized. Specific soluble apoE/Aβ complex levels were detected by ELISA as: 1) Soluble hippocampal apoE/Aβ complex was only detected using MOAB-2 as a capture antibody, as no signal was

seen when using a non-specific IgG_{2b} isotyped matched capture antibody; 2) Complex levels decreased with increased sample dilution; and 3) there were no detectable soluble complex levels in the cerebellum, a region spared of Aβ pathology in EFAD mice. These data validate soluble apoE/Aβ complex detection *in vivo* by ELISA.

Soluble apoE/Aβ complex levels are lower and less stable with APOE4.

Next, the effect of *APOE* genotype on soluble apoE/Aβ complex levels and stability was determined. ApoE/Aβ complex levels were 50% lower in E4FAD mice compared with E2FAD and E3FAD mice (Figure 2B). For apoE/Aβ complex stability (Figure 2C), complex levels were measured from the same sample in the presence of 0 %, 0.02 % or 0.2 % SDS. Complex levels were normalized to the 0 % SDS control for each paired samples set. The addition of SDS reduced apoE/Aβ complex levels, in an *APOE* genotype-specific manner. With 0.02% SDS, apoE4/Aβ complex levels were reduced by ~60% apoE3/Aβ complex levels by ~50%, and apoE2/Aβ complex levels by ~30%. The addition of 0.2% SDS further lowered complex levels in E3FAD and E4FAD mice, but not E2FAD mice. These data demonstrate that soluble hippocampal apoE/Aβ complex levels are lower and less SDS-stable in E4FAD mice compared to E3FAD and E2FAD mice and that the apoE2/Aβ complex is more stable than the apoE3/Aβ complex.

Soluble apoE/Aβ complex in synaptosomes

To determine the effect of AD and *APOE* genotype on soluble synaptic apoE/Aβ complex levels, cortical synaptosomes were isolated from control (*APOE3/3* and *APOE4/X*) and AD patients (*APOE3/3* and *APOE4/X*) (Figure 3).

ApoE/Aβ complex levels were lower in AD patients compared to controls and with APOE4 in the AD cohort

In the absence of SDS (Figure 3A), the data are normalized to *APOE3/3* controls. In the control individuals, there is no significant difference between apoE/Aβ complex levels in the *APOE3/3* and *APOE4/X*. In the AD patients, apoE/Aβ complex levels were significantly lower: 70% lower for *APOE3/3* AD patients compared to *APOE3/3* controls and 90% lower in *APOE4/X* AD patients compared to *APOE4/X* controls (Figure 3A). In addition, within the AD cohort, total apoE/Aβ complex levels were 66% lower with *APOE4/X* compared to *APOE3/3*.

To address the SDS stability of the apoE/Aβ complex (Figure 3B), complex levels were measured from the same sample in the presence of 0 % or 0.02 % SDS. ApoE/Aβ complex levels were then normalized to the 0 % SDS control for each paired sample set. In the control individuals, the addition of SDS results in a significant decrease in apoE/Aβ complex levels with *APOE4/X* compared to *APOE3/3*. ApoE/Aβ complex stability was not significantly different in the *APOE4/X* AD patients compared to *APOE3/3* AD patients. This is primarily due to the very low levels of complex present in *APOE4/X* AD samples in the absence of SDS (Figure 3A), thus after the addition of SDS, any further reduction results in values for the complex that are at the limit of detection for this ELISA. Again, this results from the pair-wise comparison between apoE/Aβ complex levels in *APOE4/X* AD patients in the absence of SDS (for example Figure 3A), where the levels of apoE/Aβ complex are already low, and apoE/Aβ complex levels in the presence of SDS (Figure 3B).

ApoE/Aβ complex in human CSF

The CSF is as an indication of the concentration of soluble proteins in the brain parenchyma. Therefore, the hypothesis that reduced levels of soluble apoE/Aβ complex and an increase in soluble oAβ levels are associated with AD and *APOE4* was tested in post-mortem CSF samples from control (*APOE3/3*) and AD patients (*APOE3/3* and *APOE4/4*).

Oligomeric Aβ levels were higher in AD patients compared to controls and significantly greater with APOE4 within the AD cohort

Recently, we described an oAβ ELISA that detects oAβ levels in EFAD mice (15), using a previously described oAβ preparation (53). For the present study, a protocol characterized by our laboratory (46) was used to produce the oAβ standard and is shown compared with fibrillar and unaggregated Aβ42 preparations (Figure 4A). As demonstrated in Figure 4A, the oAβ ELISA

demonstrates concentration-dependent detection of oAβ, with a significantly lower affinity for fibrillar Aβ42, and no detection of unaggregated Aβ42.

This ELISA was used to determine whether oAβ levels were influenced by AD diagnosis or *APOE* genotype. oAβ levels were significantly increased in AD patients compared to controls and importantly, oAβ levels were significantly greater in *APOE4/4* AD patients compared to *APOE3/3* AD patients (Figure 4B). For comparative purposes the established AD biomarkers; Aβ42 (Figure 4C), total tau (T-tau) (Figure 4D) and phosphorylated tau 181 (P-tau-181) (Figure 4E) levels were measured by ELISAs (54) in the same samples as oAβ. As expected, Aβ42 levels were significantly lower and P-tau-181 levels significantly greater in both the AD groups (*APOE3/3* and *APOE4/4*) compared to aged matched controls (*APOE3/3*). T-tau levels were significantly greater in the *APOE4/4* AD patients but not the *APOE3/3* AD patients compared to the *APOE3/3* controls. Of particular interest, in the AD group, *APOE* genotype did not affect the levels of Aβ42, T-tau or P-tau-181, all established AD biomarkers. Thus oAβ levels may play a role in AD progression, in an *APOE* genotype-specific manner.

ApoE/Aβ complex ELISA optimization for human CSF

An important consideration for measuring specific proteins in the CSF by ELISA is a standard to allow quantification of samples used on different microplates, across studies, so to allow future retrospective analysis. Although HEK-apoE is an important apoE source for biochemical studies, the relatively long sample preparation time, potential intra-laboratory differences in production quality, long term stability issues and lack of commercialization hinders routine use as an apoE/Aβ complex standard. Therefore, apoE/Aβ complex formed between recombinant apoE3, at concentrations corresponding to those in human CSF (5 μg/ml), and varied unaggregated Aβ42 concentrations, was used as a standard curve for the CSF samples (Figure 5A). Specific apoE/Aβ complex detection by ELISA in human CSF (*APOE3/3* control) was demonstrated by a high signal with capture antibody (MOAB-2) that decreased proportionately to sample dilution and no observed signal without a capture antibody, all using high bind plates to increase sensitivity (Figure 5B).

ApoE/Aβ complex levels were lower in CSF from AD patients compared to controls and importantly, significantly lower with APOE4 within the AD cohort.

ApoE/Aβ complex levels may modulate soluble oAβ levels in the CNS. The increased oAβ levels by AD and *APOE4,* raised the important question of what was the effect on apoE/Aβ complex levels. ApoE/Aβ complex levels were significantly lower in both AD cohorts compared to the control group (Figure 5C). Importantly, complex levels were significantly lower in *APOE4/4* AD patients compared to the *APOE3/3* AD patients. Thus, *APOE4* did affect the levels of oAβ (increased) and apoE/Aβ (decreased) in the AD cohort and did not affect the levels of Aβ42, T-tau or P-tau-181, suggesting oAβ and apoE/Aβ levels may play a role in AD progression. Although apoE levels were lower in AD patients compared to controls (Figure 5D), there was no correlation between apoE/Aβ complex levels and either apoE (Figure 5E, Spearman's r value 0.27, $p = 0.25$) or Aβ42 (Figure 5F, Spearman's r value 0.04, $p = 0.87$) levels in the AD patient sample set. This suggests that the levels of apoE/Aβ complex are independent of the values of its two components. Thus, apoE/Aβ complex levels are affected by both AD and *APOE* genotype.

oAβ and apoE/Aβ complex as AD biomarkers

In addition to a potential mechanistic interpretation for AD progression, oAβ and apoE/Aβ complex levels may act as AD biomarkers. As *APOE* genotype affects oAβ and apoE/Aβ complex levels, the optimal method for assessing the diagnostic potential of these markers is analysis in control and AD patients with the *APOE3/3* genotype. ROC curves were utilized to determine the predictive accuracy of each marker (Figure 6). The ROC curves are constructed by varying the threshold to classify predicted AD cases and controls. Predicted probabilities of being an AD case are calculated from marginal logistic regression models, and sensitivity (the proportion of AD cases correctly predicted, y-axis) and specificity (the proportion of AD controls

correctly predicted, i.e. true negative rate, x-axis) are calculated based on each subject's predicted case probability being above or below the varying threshold, respectively. The area under the curve (AUC) of the ROC curves is calculated, and an AUC of 0.5 demonstrates no information or diagnostic ability, whereas the higher the AUC is above 0.5, the greater the diagnostic accuracy of the biomarker. ROC analysis demonstrated the potential use of both oAβ and apoE/Aβ complex as AD biomarkers, with AUCs of 0.7 and 0.875 respectively. Next, the ROC AUCs of oAβ and apoE/Aβ were compared to the traditional AD biomarkers; Aβ42, P-tau-181 and T-tau. Aβ42 was significantly more predictive of AD (p<0.05) compared to the other markers except apoE/Aβ complex (p=0.14). Both oAβ (p=0.70) and apoE/Aβ (p=0.41) complex were as predictive for AD as P-tau-181, and apoE/Aβ was more predictive than T-tau (p<0.012). Overall, in control and AD patients with the *APOE3/3* genotype, the estimated predicative ability for AD based on the AUC values for each marker was: Aβ42 (AUC=0.98) ≥ apoE/Aβ (0.875) > P-tau-181 (0.775) ≥ oAβ (0.7) > T-tau (0.59).

DISCUSSION

For this study, a quantitative apoE/Aβ complex ELISA was developed and characterized biochemically, and then applied *in vivo* to determine the effect of *APOE* genotype and AD on soluble levels of apoE/Aβ complex and oAβ. Soluble levels of oAβ are higher and apoE/Aβ are lower with AD and specifically *APOE4*.

Biochemical data using HEK-apoE demonstrate that apoE isoform does not affect total levels of apoE/Aβ complex, but that the apoE4/Aβ complex is less stable than the apoE3/Aβ complex. By measuring total and SDS-stable apoE/Aβ complex levels, these results resolve previous contradictory *in vitro* findings (21,28,30,43). HEK-apoE has been utilized in numerous studies for apoE/Aβ complex formation (21,28). Previous data have demonstrated that HEK-apoE3, but not HEK-apoE4 form an SDS-stable apoE/Aβ complex as measured using Western analysis of SDS-PAGE (21,28,30,43). However, a corresponding value for total complex levels was not possible by Western analysis. With this new ELISA, the apoE isoforms exhibit a comparable affinity for Aβ in the absence of SDS, defined here as total apoE/Aβ complex, consistent with previous reports using non-stringent conditions to measure complex (31). The mechanism by which the apoE4/Aβ complex is less stable is unclear. ApoE4/Aβ disruption can occur by global effects on protein structure, disrupting the binding sites on the individual proteins, as well as local effects at the complex interface. ApoE4 has a lower stability and increased propensity to populate an intermediate molten globule conformation compared to the other isoforms (55,56). The apoE4/Aβ complex exhibits the lowest stability under all denaturing conditions, potentially due to the greater susceptibility of the apoE4 tertiary structure to disruption. Therefore, specific effects on the complex interface cannot be separated from effects on the stability/structure of the individual components, apoE and Aβ. An additional consideration for the stability of the apoE/Aβ complex is the effect of apoE isoform on lipoprotein lipidation. Increased lipoprotein lipidation increases the levels of SDS-stable apoE/Aβ, as determined by Western analysis of SDS-PAGE (21,22,30,43,57,58). If glial-cell derived apoE4 is less lipidated than apoE3, the apoE4/Aβ complex would be less stable (59,60). Thus, the biochemical development and characterization of the ELISA have resolved some of the inconsistencies in the apoE/Aβ complex literature. Having validated the ELISA *in vitro*, we used it *in vivo* to address the hypothesis that the levels of soluble apoE/Aβ isoform-specially modulate oAβ levels.

Soluble oAβ levels are thought to comprise the proximal neurotoxic Aβ assemblies in AD (reviewed in (61)). Soluble oAβ assemblies are neurotoxic *in vitro* and *in vivo* (61) and both soluble Aβ and oAβ correlate with disease progression in AD patients (62-65). We previously demonstrated that soluble levels of total Aβ42 and oAβ were increased in E4FAD transgenic mice compared with E2FAD and E3FAD, while the levels of apoE were comparable, suggesting a functional difference between the isoforms. In the present study, soluble apoE4/Aβ complex levels were lower than apoE2/Aβ and

apoE3/Aβ complex levels in EFAD mice. These data indicate an inverse association between apoE/Aβ complex and oAβ levels, and are consistent with previous publications that suggest that apoE/Aβ levels isoform-specifically modulate soluble Aβ (11,15). Synapse degeneration is considered a proximal cause of cognitive deficits in AD. ApoE/Aβ complex levels may affect synaptic Aβ levels and function. At the synapse, as with the whole brain, apoE/Aβ complex appears to be present as an insoluble and soluble form. IHC co-localization of apoE and Aβ at the synapse is a measure of primarily insoluble apoE/Aβ complex (35,36), and data demonstrate insoluble apoE/Aβ complex appears to form preferentially with apoE4 compared to apoE3 (36). Previous results have shown that the detergent and guanidine extraction pattern of mouse apoE parallels that of Aβ42 in 5xFAD mice (5), and the proportion of apoE/Aβ complex in insoluble fractions was increased in AD synaptosomes compared to controls (Gylys lab. unpublished observations). Importantly, insoluble apoE4/Aβ complex may accumulate in autophagic structures within synaptic terminals (66,67). However, the effect of *APOE* genotype on soluble synaptic apoE/Aβ complex levels is less clear. Soluble Aβ, soluble oAβ, P-tau and SDS-stable P-tau oligomers (37-39,68) are detected in AD synaptosomes, and data presented herein also demonstrate the presence of soluble apoE/Aβ complex in AD synaptososomes, with levels reduced compared to controls. Soluble apoE/Aβ complex levels were also lower in synaptosomes from AD patients with *APOE4* compared to *APOE3*. These data indicate a difference in apoE/Aβ complex solubility during disease progression, which may lead to alterations in synaptic Aβ trafficking or clearance.

Although the cellular process by which apoE isoform modulates soluble Aβ pathology is unclear, a number of apoE/Aβ complex-based mechanisms have been proposed. Examples include effects on: 1) Aβ oligomerization (69,70); 2) Aβ clearance via glia (71-74), neurons (75,76), and/or the blood-brain barrier (77,78); 3) enzymatic degradation (57); and 4) drainage via the interstitial fluid (ISF) (16) or perivasculature (79). Furthermore, the dynamic compartmentalization of Aβ in the CNS has been identified as an important factor in regulating the level of soluble Aβ (80), which may be affected by and/or affect apoE/Aβ complex. Importantly, the levels of Aβ in each compartment affect the equilibrium between compartments, again with further modulation by the apoE isoforms. To understand this process, new techniques have been developed to determine apoE and Aβ turnover via stable isotope-labeling kinetics (SILK) (81) and microdialysis of ISF (80). In addition, Hong, Selkoe and co-workers have recently identified Aβ in biochemically distinct compartments in the brain, including an ISF pool, a TBS-extractable pool, an SDS-extractable pool and an insoluble or plaque pool (80). In FAD-Tg mice with a high plaque burden, ISF Aβ appears to be rapidly sequestered in a TBS soluble pool (80). Overall, the majority of Aβ in the ISF originates from a less soluble parenchymal Aβ pool rather than from production (80). ApoE isoform-specific apoE/Aβ complex levels could affect the dynamic compartmentalization of Aβ through the mechanisms discussed above. For example, with *APOE3,* high levels of soluble apoE/Aβ complex may reduce soluble and oAβ levels via clearance. With *APOE4*, low levels of soluble apoE/Aβ complex may result in increased soluble Aβ levels, particularly oAβ. Alternatively, if apoE is acting as a pathologic chaperone for soluble Aβ, reducing the level or stability of apoE/Aβ complex may decrease oAβ levels (24,82). As described herein, the ability to detect apoE isoform-specific differences in the levels of soluble oAβ and apoE/Aβ complex levels *in vivo* is a critical step in identifying the mechanism by which the apoE isoforms modulate soluble Aβ pathology.

As with human synaptosomes, in human CSF levels of soluble oAβ were greater and apoE/Aβ lower with *APOE4* compared to *APOE3* in the AD cohort. The ability of both oAβ and apoE/Aβ to distinguish between *APOE3/3* and *APOE4/4* AD patients is consistent with the increased risk and earlier age of disease onset with *APOE4*, highlighting the potential for these markers to track disease progression. In addition, apoE/Aβ and oAβ may represent novel CSF biomarkers, an important focus for AD research (54). In control and AD patients with the *APOE3/3* genotype both oAβ and apoE/Aβ complex diagnosed AD with

the same accuracy as P-tau-181, a currently accepted AD biomarker. Furthermore, as oAβ and apoE/Aβ are based on potential mechanisms of AD progression, both represent biomarkers to assess therapeutic efficacy *in vivo* and in clinical trials. Currently, drug trials targeting oAβ and apoE/Aβ complex are either in the preclinical phase or underway. For Aβ, therapies include both passive and active Aβ immunotherapy, BACE inhibitors, γ-secretase inhibitors and γ-secretase modulators. Aside from measures of cognition, neuroimaging for amyloid with Pittsburgh compound B and CSF biomarkers such as Aβ42 and P-tau levels are the only biomarkers available to determine drug efficacy (83). Given that amyloid plaques appear not to correlate with dementia and may not represent the ideal target, and it is unclear whether low CSF Aβ42 levels will be reversible with long-term treatment, the relevance of these biomarkers for therapeutic trials is unclear. oAβ levels represent a novel biomarker to monitor drug efficacy. For apoE/Aβ complex, therapies are in development that disrupt (24,82) or increase (84) apoE/Aβ complex levels. Examples include RXR, LXR and PPARγ agonists, which increase the levels and lipidation state of apoE (57,84-86), apoE structural correctors (87), and Aβ12-28P that blocks apoE/Aβ interactions (24,82). However, there are no data on whether these drugs will affect apoE/Aβ complex levels *in vivo*, and more importantly, the effects of these therapeutic interventions on the human apoE isoforms are unknown. The data presented here indicate that increasing soluble levels of apoE/Aβ is a therapeutic target, as it will reduce oAβ levels. Importantly the efficacy of therapeutic treatments targeting soluble levels of oAβ and apoE/Aβ complex can now be determined using the ELISAs described herein.

Acknowledgements

This work was supported, in whole or in part, by National Institutes of Health Grants P01AG030128 (through the NIA) (to M.J.L. and S.E.), AG27465 (to KHG), and by AG18879 (to CAM); Alzheimer's Association Grant ZEN-08-899000 (to M.J.L.); University of Illinois at Chicago Center for Clinical and Translational Science Grant UL1RR029879 (to M.J.L.); and an Alzheimer's drug discovery foundation grant (M.J.L and S.E). HVV is supported by the Daljit S. and Elaine Sarkaria Chair in Diagnostic Medicine. Human post-mortem samples were obtained from the Alzheimer's Disease Research Center Neuropathology Cores of USC (NIA 050 AG05142), UCLA (NIA P50 AG 16970), and UC Irvine (NIA P50 AG016573). Human CSF samples were obtained from the University of Kentucky Alzheimer's Disease Research Center, NIA P30 AG028383). The authors also gratefully acknowledge Maria Corrada and Claudia Kawas and the 90+ Study for providing tissue (UC Irvine; PI CK, Co-I MC).

FOOTNOTES

[1] **Abbreviations:** Aβ, amyloid-β; apoE, apolipoprotein E; AD, Alzheimer's disease; AUC, area under the curve; CSF, cerebrospinal fluid; FAD, familial AD; FAD-Tg, transgenic mice expressing FAD mutations; IHC, immunohistochemistry; 5xFAD mice, FAD-Tg which co-express 5 FAD mutations; oAβ, oligomeric amyloid-β; ROC; receiver operating characteristic curves; SEC, size exclusion chromatography; SDS-PAGE; sodium dodecyl sulphate polyacrylamide gel electrophoresis; Tg, transgenic; T-tau, total tau; P-tau-181, phosphorylated tau at residue 181.

REFERENCES

1. Verghese, P. B., Castellano, J. M., and Holtzman, D. M. (2011) *Lancet Neurol* **10**, 241-252
2. Bu, G. (2009) *Nat Rev Neurosci* **10**, 333-344
3. Hardy, J. A., and Higgins, G. A. (1992) *Science* **256**, 184-185.
4. Wisniewski, T., and Frangione, B. (1992) *Neurosci Lett* **135**, 235-238
5. Youmans, K. L., Leung, S., Zhang, J., Maus, E., Baysac, K., Bu, G., Vassar, R., Yu, C., and Ladu, M. J. (2011) *J Neurosci Methods* **196**, 51-59
6. Strittmatter, W. J., Saunders, A. M., Goedert, M., Weisgraber, K. H., Dong, L. M., Jakes, R., Huang, D. Y., Pericak-Vance, M., Schmechel, D., and Roses, A. D. (1994) *Proc Natl Acad Sci U S A* **91**, 11183-11186
7. Strittmatter, W. J., Saunders, A. M., Schmechel, D., Pericak-Vance, M., Enghild, J., Salvesen, G. S., and Roses, A. D. (1993) *Proc Natl Acad Sci U S A* **90**, 1977-1981
8. Drzezga, A., Grimmer, T., Henriksen, G., Muhlau, M., Perneczky, R., Miederer, I., Praus, C., Sorg, C., Wohlschlager, A., Riemenschneider, M., Wester, H. J., Foerstl, H., Schwaiger, M., and Kurz, A. (2009) *Neurology* **72**, 1487-1494
9. Grimmer, T., Tholen, S., Yousefi, B. H., Alexopoulos, P., Forschler, A., Forstl, H., Henriksen, G., Klunk, W. E., Mathis, C. A., Perneczky, R., Sorg, C., Kurz, A., and Drzezga, A. (2010) *Biol Psychiatry* **68**, 879-884
10. Jones, P. B., Adams, K. W., Rozkalne, A., Spires-Jones, T. L., Hshieh, T. T., Hashimoto, T., von Armin, C. A., Mielke, M., Bacskai, B. J., and Hyman, B. T. (2011) *PloS one* **6**, e14586
11. Bales, K. R., Liu, F., Wu, S., Lin, S., Koger, D., DeLong, C., Hansen, J. C., Sullivan, P. M., and Paul, S. M. (2009) *The Journal of neuroscience* **29**, 6771-6779
12. Haass, C., and Selkoe, D. J. (2007) *Nat Rev Mol Cell Biol* **8**, 101-112
13. Hardy, J. (2006) *J Alzheimers Dis* **9**, 151-153
14. Larson, M. E., and Lesne, S. E. (2012) *J Neurochem* **120 Suppl 1**, 125-139
15. Youmans, K. L., Tai, L. M., Nwabuisi-Heath, E., Jungbauer, L., Kanekiyo, T., Gan, M., Kim, J., Eimer, W. A., Estus, S., Rebeck, G. W., Weeber, E. J., Bu, G., Yu, C., and Ladu, M. J. (2012) *The Journal of biological chemistry*
16. Castellano, J. M., Kim, J., Stewart, F. R., Jiang, H., DeMattos, R. B., Patterson, B. W., Fagan, A. M., Morris, J. C., Mawuenyega, K. G., Cruchaga, C., Goate, A. M., Bales, K. R., Paul, S. M., Bateman, R. J., and Holtzman, D. M. (2011) *Sci Transl Med* **3**, 89ra57
17. Aleshkov, S., Abraham, C. R., and Zannis, V. I. (1997) *Biochemistry* **36**, 10571-10580
18. Bentley, N. M., LaDu, M. J., Rajan, C., Getz, G. S., and Reardon, C. A. (2002) *Biochem J* **366**, 273-279
19. Golabek, A., Marques, M. A., Lalowski, M., and Wisniewski, T. (1995) *Neurosci Lett* **191**, 79-82
20. Golabek, A. A., Soto, C., Vogel, T., and Wisniewski, T. (1996) *J. Biol. Chem.* **271**, 10602-10606
21. LaDu, M. J., Falduto, M. T., Manelli, A. M., Reardon, C. A., Getz, G. S., and Frail, D. E. (1994) *The Journal of biological chemistry* **269**, 23403-23406

22. LaDu, M. J., Lukens, J. R., Reardon, C. A., and Getz, G. S. (1997) *J Neurosci Res* **49**, 9-18
23. Pillot, T., Goethals, M., Vanloo, B., Lins, L., Brasseur, R., Vandekerckhove, J., and Rosseneu, M. (1997) *Euro. J. Biochem.* **243**, 650-659
24. Sadowski, M., Pankiewicz, J., Scholtzova, H., Ripellino, J. A., Li, Y., Schmidt, S. D., Mathews, P. M., Fryer, J. D., Holtzman, D. M., Sigurdsson, E. M., and Wisniewski, T. (2004) *Am J Pathol* **165**, 937-948
25. Yamauchi, K., Tozuka, M., Hidaka, H., Nakabayashi, T., Sugano, M., Kondo, Y., Nakagawara, A., and Katsuyama, T. (2000) *J Neurosci Res* **62**, 608-614
26. Yang, D. S., Smith, J. D., Zhou, Z., Gandy, S. E., and Martins, R. N. (1997) *Journal of neurochemistry* **68**, 721-725
27. Zhou, Z., Smith, J. D., Greengard, P., and Gandy, S. (1996) *Molecular medicine (Cambridge, Mass* **2**, 175-180
28. LaDu, M. J., Pederson, T. M., Frail, D. E., Reardon, C. A., Getz, G. S., and Falduto, M. T. (1995) *The Journal of biological chemistry* **270**, 9039-9042
29. Strittmatter, W. J., Weisgraber, K. H., Huang, D. Y., Dong, L. M., Salvesen, G. S., Pericak-Vance, M., Schmechel, D., Saunders, A. M., Goldgaber, D., and Roses, A. D. (1993) *Proceedings of the National Academy of Sciences of the United States of America* **90**, 8098-8102
30. LaDu, M. J., Munson, G. W., Jungbauer, L., Getz, G. S., Reardon, C. A., Tai, L. M., and Yu, C. (2012) *Biochim Biophys Acta - Molecular and Cell Biology of Lipids* **1821**, 295-302
31. Morikawa, M., Fryer, J. D., Sullivan, P. M., Christopher, E. A., Wahrle, S. E., DeMattos, R. B., O'Dell, M. A., Fagan, A. M., Lashuel, H. A., Walz, T., Asai, K., and Holtzman, D. M. (2005) *Neurobiol Dis* **19**, 66-76
32. Manelli, A. M., Stine, W. B., Van Eldik, L. J., and LaDu, M. J. (2004) *J Mol Neurosci* **23**, 235-246
33. Russo, C., Angelini, G., Dapino, D., Piccini, A., Piombo, G., Schettini, G., Chen, S., Teller, J. K., Zaccheo, D., Gambetti, P., and Tabaton, M. (1998) *Proc. Natl. Acad. Sci. USA* **95**, 15598-15602
34. Zhou, Z., Relkin, N., Ghiso, J., Smith, J. D., and Gandy, S. (2002) *Mol Med* **8**, 376-381
35. Arold, S., Sullivan, P., Bilousova, T., Teng, E., Miller, C. A., Poon, W. W., Vinters, H. V., Cornwell, L. B., Saing, T., Cole, G. M., and Gylys, K. H. (2012) *Acta neuropathologica* **123**, 39-52
36. Koffie, R. M., Hashimoto, T., Tai, H. C., Kay, K. R., Serrano-Pozo, A., Joyner, D., Hou, S., Kopeikina, K. J., Frosch, M. P., Lee, V. M., Holtzman, D. M., Hyman, B. T., and Spires-Jones, T. L. (2012) *Brain : a journal of neurology* **135**, 2155-2168
37. Henkins, K. M., Sokolow, S., Miller, C. A., Vinters, H. V., Poon, W. W., Cornwell, L. B., Saing, T., and Gylys, K. H. (2012) *Brain Pathol* **22**, 826-833
38. Gylys, K. H., Fein, J. A., Yang, F., Wiley, D. J., Miller, C. A., and Cole, G. M. (2004) *Am J Pathol* **165**, 1809-1817
39. Fein, J. A., Sokolow, S., Miller, C. A., Vinters, H. V., Yang, F., Cole, G. M., and Gylys, K. H. (2008) *Am J Pathol* **172**, 1683-1692

40. Gylys, K. H., Fein, J. A., Yang, F., Miller, C. A., and Cole, G. M. (2007) *Neurobiology of aging* **28**, 8-17
41. Youmans, K. L., Tai, L. M., Kanekiyo, T., Stine, W. B., Jr., Michon, S. C., Nwabuisi-Heath, E., Manelli, A., Fu, Y., Riordan, S., Eimer, W. A., Binder, L., Bu, G., Yu, C., Hartley, D. M., and Ladu, M. J. (2012) *Molecular neurodegeneration* **7**, 8
42. Munson, G. W., Roher, A. E., Kuo, Y. M., Gilligan, S. M., Reardon, C. A., Getz, G. S., and LaDu, M. J. (2000) *Biochemistry* **39**, 16119-16124
43. LaDu, M. J., Stine, W. B., Jr., Narita, M., Getz, G. S., Reardon, C. A., and Bu, G. (2006) *Biochemistry* **45**, 381-390
44. Dahlgren, K. N., Manelli, A. M., Stine, W. B., Jr., Baker, L. K., Krafft, G. A., and LaDu, M. J. (2002) *The Journal of biological chemistry* **277**, 32046-32053
45. Stine, W. B., Jr., Dahlgren, K. N., Krafft, G. K., and LaDu, M. J. (2003) *The Journal of biological chemistry* **278**, 11612-11622
46. Stine, W. B., Jungbauer, L., Yu, C., and LaDu, M. J. (2011) *Methods Mol Biol* **670**, 13-32
47. (1997) *Neurobiology of aging* **18**, S1-2
48. Nelson, P. T., Braak, H., and Markesbery, W. R. (2009) *Journal of neuropathology and experimental neurology* **68**, 1-14
49. Robin, X., Turck, N., Hainard, A., Tiberti, N., Lisacek, F., Sanchez, J. C., and Muller, M. (2011) *BMC bioinformatics* **12**, 77
50. Team, C. (2012) *Vienna, Austria. ISBN 3-900051-07-0, URL* http://www.R-project.org
51. DeLong, E. R., DeLong, D. M., and Clarke-Pearson, D. L. (1988) *Biometrics* **44**, 837-845
52. Findlay, J. W., and Dillard, R. F. (2007) *The AAPS journal* **9**, E260-267
53. Moore, B. D., Rangachari, V., Tay, W. M., Milkovic, N. M., and Rosenberry, T. L. (2009) *Biochemistry* **48**, 11796-11806
54. Shoji, M. (2011) *Int J Alzheimers Dis* **2011**, 564321
55. Morrow, J. A., Hatters, D. M., Lu, B., Hochtl, P., Oberg, K. A., Rupp, B., and Weisgraber, K. H. (2002) *The Journal of biological chemistry* **277**, 50380-50385
56. Morrow, J. A., Segall, M. L., Lund-Katz, S., Phillips, M. C., Knapp, M., Rupp, B., and Weisgraber, K. H. (2000) *Biochemistry* **39**, 11657-11666
57. Jiang, Q., Lee, C. Y., Mandrekar, S., Wilkinson, B., Cramer, P., Zelcer, N., Mann, K., Lamb, B., Willson, T. M., Collins, J. L., Richardson, J. C., Smith, J. D., Comery, T. A., Riddell, D., Holtzman, D. M., Tontonoz, P., and Landreth, G. E. (2008) *Neuron* **58**, 681-693
58. Hirsch-Reinshagen, V., Maia, L. F., Burgess, B. L., Blain, J. F., Naus, K. E., McIsaac, S. A., Parkinson, P. F., Chan, J. Y., Tansley, G. H., Hayden, M. R., Poirier, J., Van Nostrand, W., and Wellington, C. L. (2005) *The Journal of biological chemistry* **280**, 43243-43256
59. Gong, J. S., Kobayashi, M., Hayashi, H., Zou, K., Sawamura, N., Fujita, S. C., Yanagisawa, K., and Michikawa, M. (2002) *The Journal of biological chemistry* **31**, 31
60. Riddell, D. R., Zhou, H., Atchison, K., Warwick, H. K., Atkinson, P. J., Jefferson, J., Xu, L., Aschmies, S., Kirksey, Y., Hu, Y., Wagner, E., Parratt, A., Xu, J., Li,

Z., Zaleska, M. M., Jacobsen, J. S., Pangalos, M. N., Reinhart, P. H., Riddell, D. R., Zhou, H., Atchison, K., Warwick, H. K., Atkinson, P. J., Jefferson, J., Xu, L., Aschmies, S., Kirksey, Y., Hu, Y., Wagner, E., Parratt, A., Xu, J., Li, Z., Zaleska, M. M., Jacobsen, J. S., Pangalos, M. N., and Reinhart, P. H. (2008) *Journal of Neuroscience* **28**, 11445-11453
61. Walsh, D. M., and Teplow, D. B. (2012) *Prog Mol Biol Transl Sci* **107**, 101-124
62. Kuo, Y. M., Emmerling, M. R., Vigo-Pelfrey, C., Kasunic, T. C., Kirkpatrick, J. B., Murdoch, G. H., Ball, M. J., and Roher, A. E. (1996) *J. Biol. Chem.* **271**, 4077-4081
63. Selkoe, D. J. (2011) *Nat Med* **17**, 1060-1065
64. Tomic, J. L., Pensalfini, A., Head, E., and Glabe, C. G. (2009) *Neurobiology of disease* **35**, 352-358
65. Jin, M., Shepardson, N., Yang, T., Chen, G., Walsh, D., and Selkoe, D. J. (2011) *Proc Natl Acad Sci U S A* **108**, 5819-5824
66. Nixon, R. A. (2007) *Journal of cell science* **120**, 4081-4091
67. Li, J., Kanekiyo, T., Shinohara, M., Zhang, Y., Ladu, M. J., Xu, H., and Bu, G. (2012) *The Journal of biological chemistry*
68. Sokolow, S., Henkins, K. M., Bilousova, T., Miller, C. A., Vinters, H. V., Poon, W., Cole, G. M., and Gylys, K. H. (2012) *Neurobiology of aging* **33**, 1545-1555
69. Cerf, E., Gustot, A., Goormaghtigh, E., Ruysschaert, J. M., and Raussens, V. (2011) *FASEB J* **25**, 1585-1595
70. Petrlova, J., Hong, H. S., Bricarello, D. A., Harishchandra, G., Lorigan, G. A., Jin, L. W., and Voss, J. C. (2011) *Proteins* **79**, 402-416
71. Koistinaho, M., Lin, S., Wu, X., Esterman, M., Koger, D., Hanson, J., Higgs, R., Liu, F., Malkani, S., Bales, K. R., and Paul, S. M. (2004) *Nat Med* **10**, 719-726
72. Mandrekar, S., Jiang, Q., Lee, C. Y., Koenigsknecht-Talboo, J., Holtzman, D. M., and Landreth, G. E. (2009) *The Journal of neuroscience : the official journal of the Society for Neuroscience* **29**, 4252-4262
73. Basak, J. M., Verghese, P. B., Yoon, H., Kim, J., and Holtzman, D. M. (2012) *The Journal of biological chemistry* **287**, 13959-13971
74. Thal, D. R. (2012) *Exp Neurol* **236**, 1-5
75. Vekrellis, K., Ye, Z., Qiu, W. Q., Walsh, D., Hartley, D., Chesneau, V., Rosner, M. R., and Selkoe, D. J. (2000) *Journal of Neuroscience* **20**, 1657-1665
76. Wirths, O., and Bayer, T. A. (2012) *Life sciences* **91**, 1148-1152
77. Deane, R., Sagare, A., Hamm, K., Parisi, M., Lane, S., Finn, M. B., Holtzman, D. M., and Zlokovic, B. V. (2008) *J Clin Invest* **118**, 4002-4013
78. Bachmeier, C., Beaulieu-Abdelahad, D., Crawford, F., Mullan, M., and Paris, D. (2012) *J Mol Neurosci*
79. Hawkes, C. A., Sullivan, P. M., Hands, S., Weller, R. O., Nicoll, J. A., and Carare, R. O. (2012) *PloS one* **7**, e41636
80. Hong, S., Quintero-Monzon, O., Ostaszewski, B. L., Podlisny, D. R., Cavanaugh, W. T., Yang, T., Holtzman, D. M., Cirrito, J. R., and Selkoe, D. J. (2011) *The Journal of neuroscience : the official journal of the Society for Neuroscience* **31**, 15861-15869

81. Basak, J. M., Kim, J., Pyatkivskyy, Y., Wildsmith, K. R., Jiang, H., Parsadanian, M., Patterson, B. W., Bateman, R. J., and Holtzman, D. M. (2012) *Molecular neurodegeneration* **7**, 14
82. Sadowski, M. J., Pankiewicz, J., Scholtzova, H., Mehta, P. D., Prelli, F., Quartermain, D., and Wisniewski, T. (2006) *Proceedings of the National Academy of Sciences of the United States of America* **103**, 18787-18792
83. Morris, J. C., and Selkoe, D. J. (2011) *Neurobiology of aging* **32 Suppl 1**, S1-3
84. Cramer, P. E., Cirrito, J. R., Wesson, D. W., Lee, C. Y., Karlo, J. C., Zinn, A. E., Casali, B. T., Restivo, J. L., Goebel, W. D., James, M. J., Brunden, K. R., Wilson, D. A., and Landreth, G. E. (2012) *Science* **335**, 1503-1506
85. Lefterov, I., Bookout, A., Wang, Z., Staufenbiel, M., Mangelsdorf, D., and Koldamova, R. (2007) *Molecular neurodegeneration* **2**, 20
86. Terwel, D., Steffensen, K. R., Verghese, P. B., Kummer, M. P., Gustafsson, J. A., Holtzman, D. M., and Heneka, M. T. (2011) *The Journal of neuroscience : the official journal of the Society for Neuroscience* **31**, 7049-7059
87. Mahley, R. W., and Huang, Y. (2012) *Journal of medicinal chemistry* **55**, 8997-9008

FIGURE LEGENDS

Figure 1. Biochemical characterization of apoE/Aβ complex ELISA with HEK-apoE and synthetic Aβ.

(A) Total apoE/Aβ complex levels for each apoE isoform with HEK-apoE fixed at 30.0 nM, and unaggregated Aβ42 varied from 0.15-150.0 nM. **(B)** Total level of apoE/Aβ complex for each apoE isoform with unaggregated Aβ42 fixed at 3.0 nM and HEK-apoE varied from 1.5-1500.0 nM. **(C)** Stability of apoE/Aβ complex in the presence of SDS from 0-2%. **(D)** Stability of apoE/Aβ complex at varied pH. For all experiments n = 5 with duplicate samples. Data are expressed as mean ± SEM, analysed by one-way ANOVA with Tukey's multiple comparison post-hoc analysis. $^{*}p < 0.05$ compared to apoE3, $^{\#}p < 0.05$ compared to apoE2.

Figure 2. ApoE/Aβ complex levels and stability in soluble brain extracts from EFAD mice.

(A) Standardization and control for apoE/Aβ complex levels in the soluble (TBS) extraction fraction from the hippocampus and cerebellum of E3FAD mice at 6 months. **(B)** ApoE/Aβ complex in the soluble extraction fraction from the hippocampus of E2FAD, E3FAD and E4FAD mice at 6 months. **(C)** Soluble apoE/Aβ complex stability in 0.02 % and 0.2 % SDS in samples as described for **(B)**. Standard curve for apoE/Aβ ELISA: 140.0nM HEK-apoE3 with 0.15-50.0nM unaggregated Aβ42. For all experiments n = 8 with duplicate samples. Data are expressed as mean ± SEM, and were analysed by one-way analysis of variance (ANOVA) followed by Tukey's post-hoc analysis, (Figures 2B) or by two-way ANOVA followed by Bonferroni post hoc analysis (Figure 2C). $^{*}p < 0.05$.

Figure 3. Soluble apoE/Aβ complex levels and stability in synaptosome-enriched extracts from human cortex.

(A) and **(B)** were measured in aged matched control subjects (*APOE3/3* and *APOE4/X*) and Alzheimer's disease (AD) patients (*APOE3/3* and *APOE4/X*). Description of sample groups in Supplemental Table 1. **(A)** ApoE/Aβ complex levels in cortical synaptosomes (P-2 fraction). Controls: n = 10 *APOE3/3*, n =7 *APOE4/X*; AD: n = 9 *APOE3/3*, n =7 *APOE4/X*. **(B)** ApoE/Aβ complex stability in 0.02% SDS. Standard curve for apoE/Aβ ELISA in human synaptosome-enriched extracts: 14.0 nM HEK-apoE3 with 0.86-450.0 nM unaggregated Aβ42. Controls: n = 5 *APOE3/3*, n =5 *APOE4/X*; AD: n = 6 *APOE3/3*, n =5 *APOE4/X*. Data are expressed as mean ± SEM, analysed by one-way ANOVA followed by Tukey's multiple comparison post-hoc analysis. $^{*}p < 0.05$.

Figure 4. Oligomeric Aβ in human CSF compared with Aβ42, total tau (T-tau) and phosphorylated tau 181 (P-tau-181).

(A) Standard curve for oligomeric Aβ ELISA: 0-500 ng/ml of oligomeric-, fibrillar- and unaggregated-Aβ42 preparations. **B - E** were measured in the CSF from age matched control subjects (*APOE3/3*) and AD patients (*APOE3/3* and *APOE4/4*). Description of sample groups in Supplemental Table 2. **(B)** oAβ. **(C)** Aβ42, **(D)** total tau (T-tau) and **(E)** phosho-tau-181 (P-tau181). Innotest® kits by Innogenetics for Aβ42, T-tau and P-tau-181. For all experiments n = 10 with duplicate samples. Data are expressed as mean ± SEM, analysed by one-way ANOVA followed by Tukey's multiple comparison post-hoc analysis. $^{*}p < 0.05$. L.O.D = Limit of detection.

Figure 5. ApoE/Aβ complex levels in human CSF.

(A) Standard curve for apoE/Aβ ELISA in human CSF: 5 μg/ml recombinant apoE3 with 0.15-50.0 ng/ml unaggregated Aβ42. **(B)** Specific apoE/Aβ complex detection by ELISA in control human *APOE3/3* CSF. The standards and CSF samples were diluted 2- to 16-fold and apoE/Aβ

complex levels measured. **(C)** ApoE/Aβ complex and **(D)** apoE levels were measured in aged matched control subjects (*APOE3/3*) and Alzheimer's disease (AD) patients (*APOE3/3* and *APOE4/4*). Description of sample groups in Supplemental Table 2. For all experiments n = 10 with duplicate samples. Data are expressed as mean ± SEM, analysed by one-way ANOVA followed by Tukey's multiple comparison post-hoc analysis. $^{*}p < 0.05$. L.O.D = Limit of detection. Spearman's correlation analysis between apoE/Aβ complex and **(E)** apoE or **(F)** Aβ42 in CSF of AD patients (*APOE3/3* and *APOE4/4*).

Figure 6. AD prediction by Aβ42, oAβ, apoE/Aβ complex, T-tau and P-tau-181 in human CSF using ROC curves.

Receiver operating characteristic (ROC) curves for Aβ42, oAβ, apoE/Aβ complex, T-tau and P-tau-181 in control and AD patients with the *APOE3/3* genotype in human CSF. ROC curves represent the predicted probabilities of being an AD case using marginal logistic regression models. Specificity (true negative rate, the proportion of AD controls correctly predicted) is plotted on the x-axis and sensitivity (the proportion of AD cases correctly predicted) is plotted on the y-axis, as calculated based on each subject's predicted case probability being above or below the varying threshold, respectively.

Figure 1. Biochemical characterization of apoE/Aβ ELISA with HEK-apoE and synthetic Aβ42

A. ApoE/Aβ complex levels

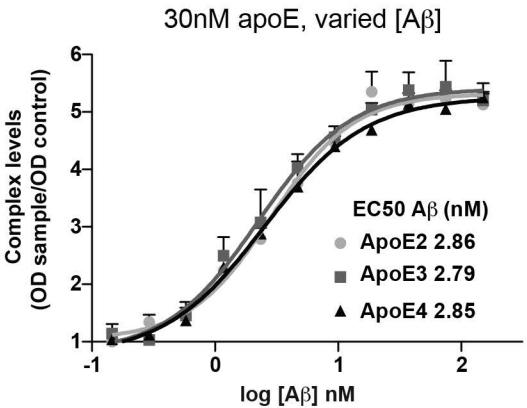

B. ApoE/Aβ complex levels

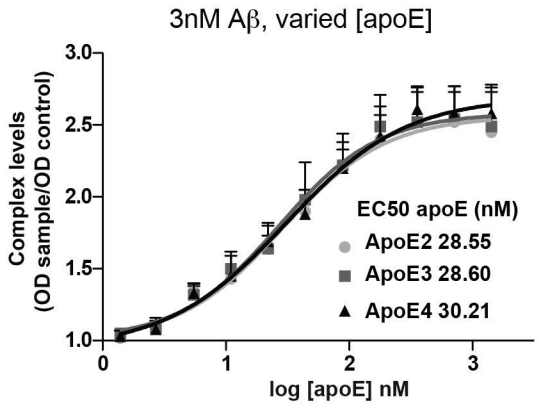

C. ApoE/Aβ complex stability: SDS

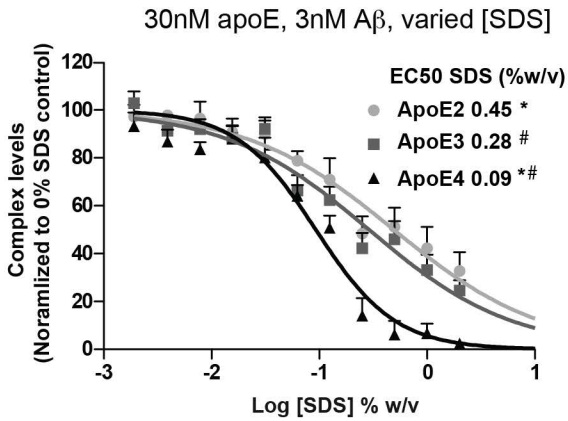

D. ApoE/Aβ complex stability: pH

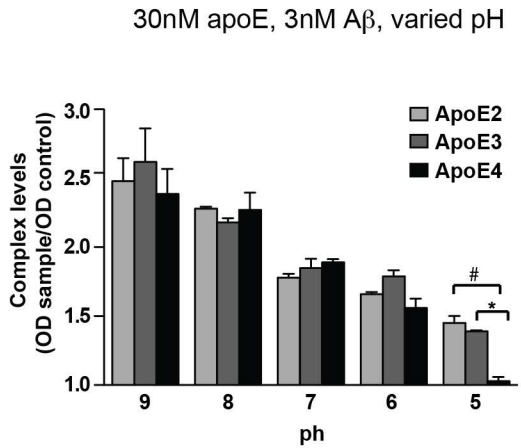

Figure 2. ApoE/Aβ complex levels in soluble brain extracts from EFAD mice

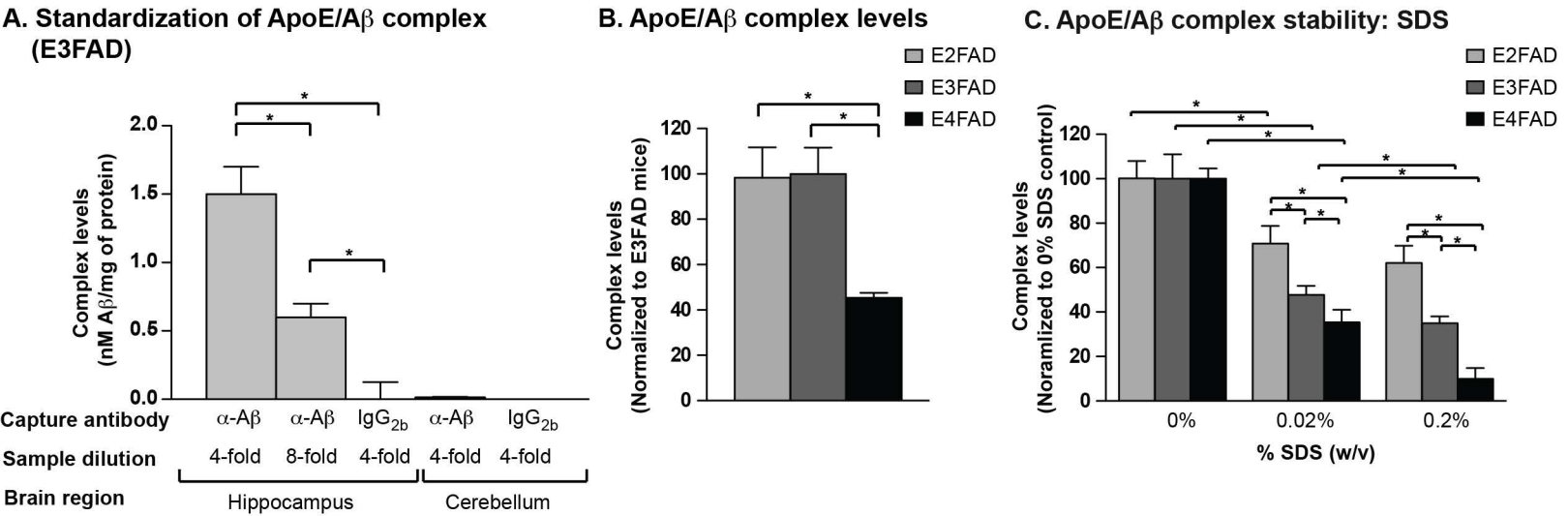

Figure 3. ApoE/Aβ complex levels in synaptosome enriched extracts from human brain tissue

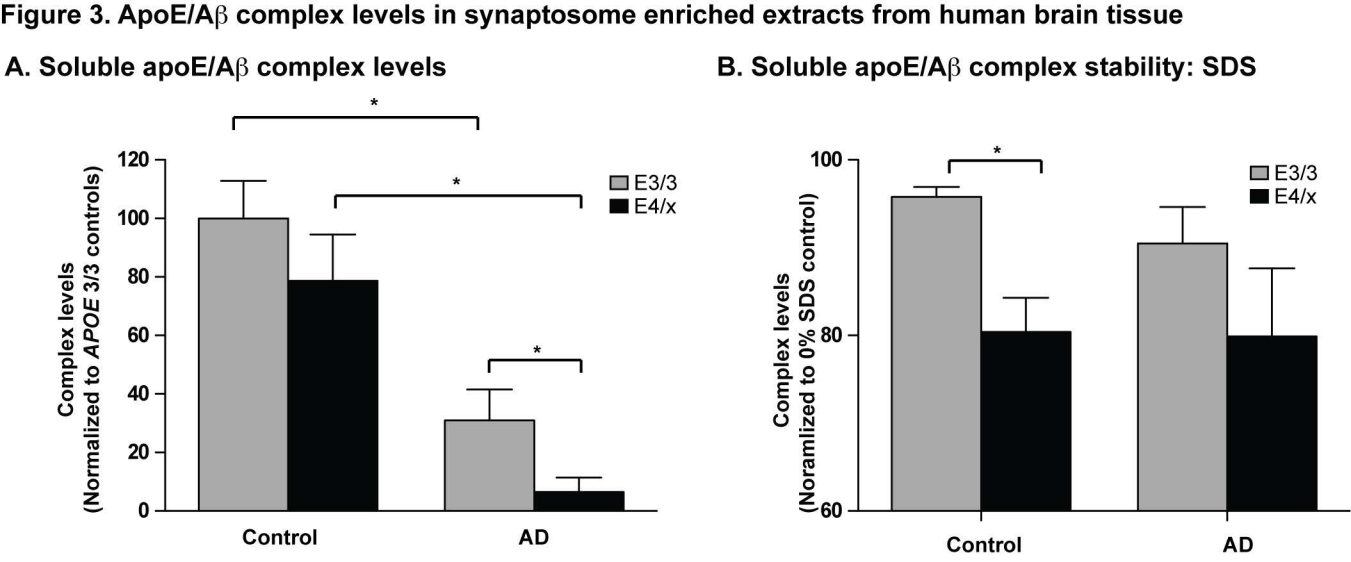

Figure 4. Oligomeric Aβ, Aβ42, Total tau, and phosphorylated tau 181 in human CSF

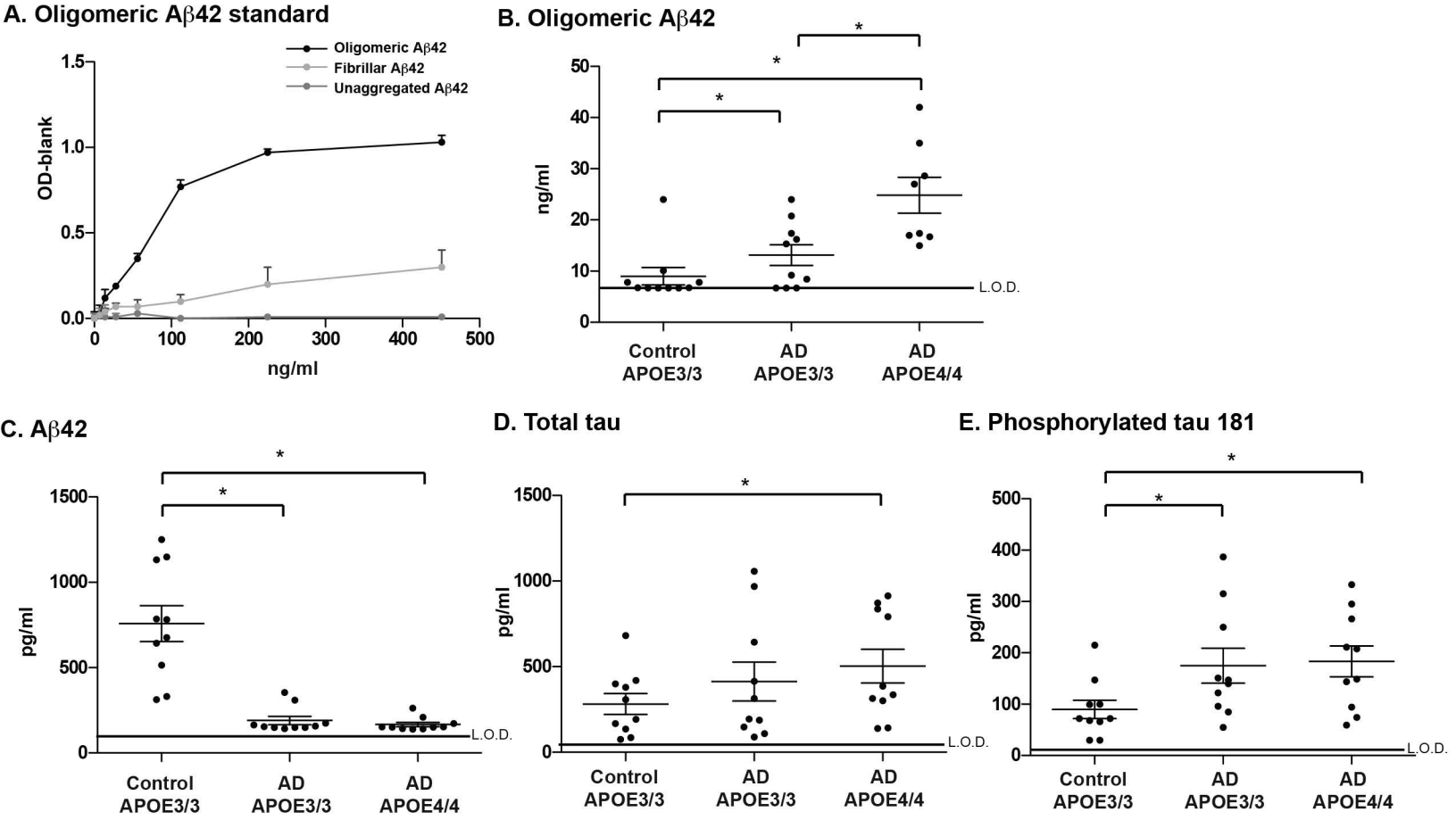

Figure 5. ApoE/Aβ complex levels in human CSF

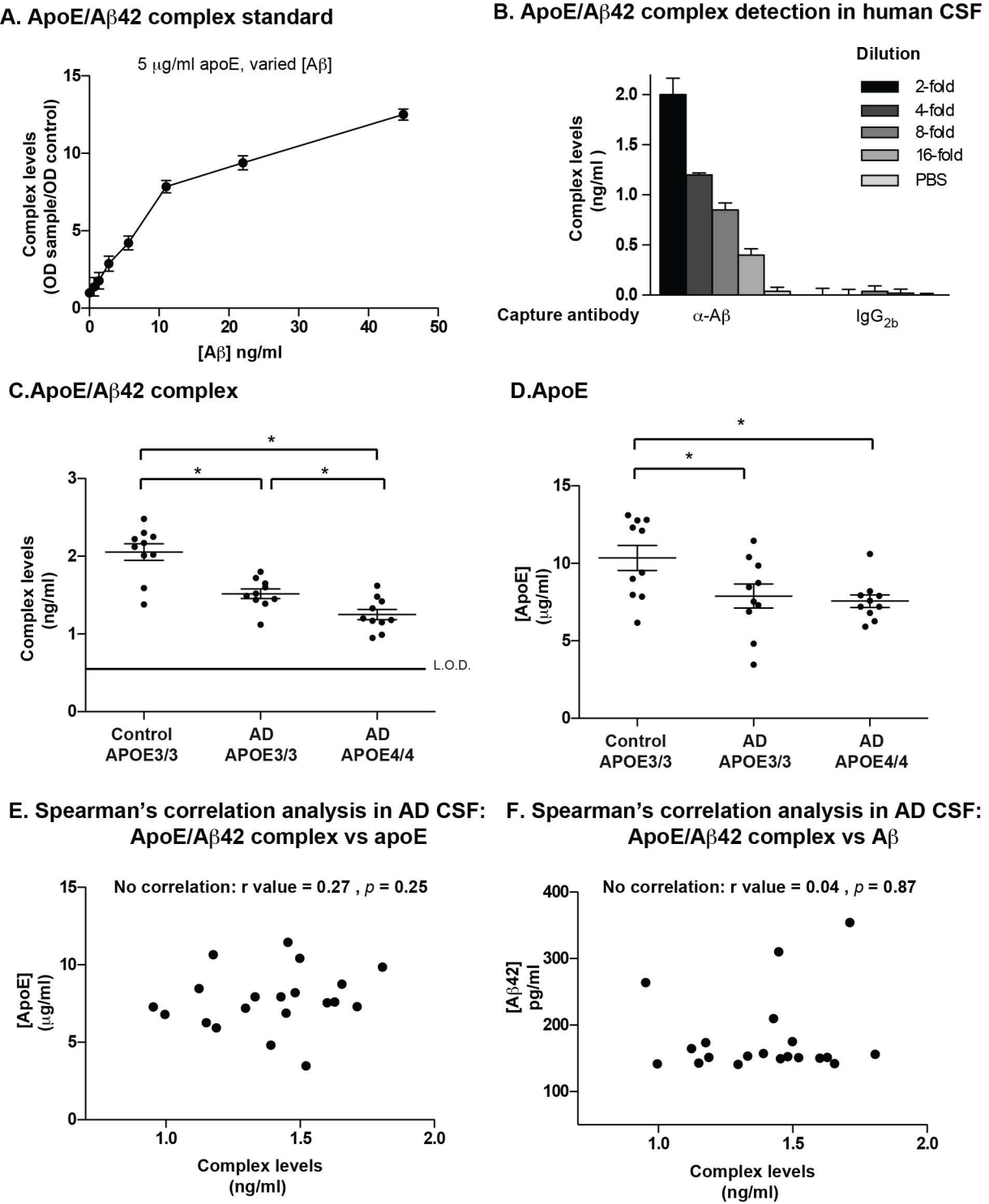

Figure 6. AD prediction by Aβ42, apoE/Aβ, Ptau-181, oAβ, and Ttau in human CSF using ROC curves.

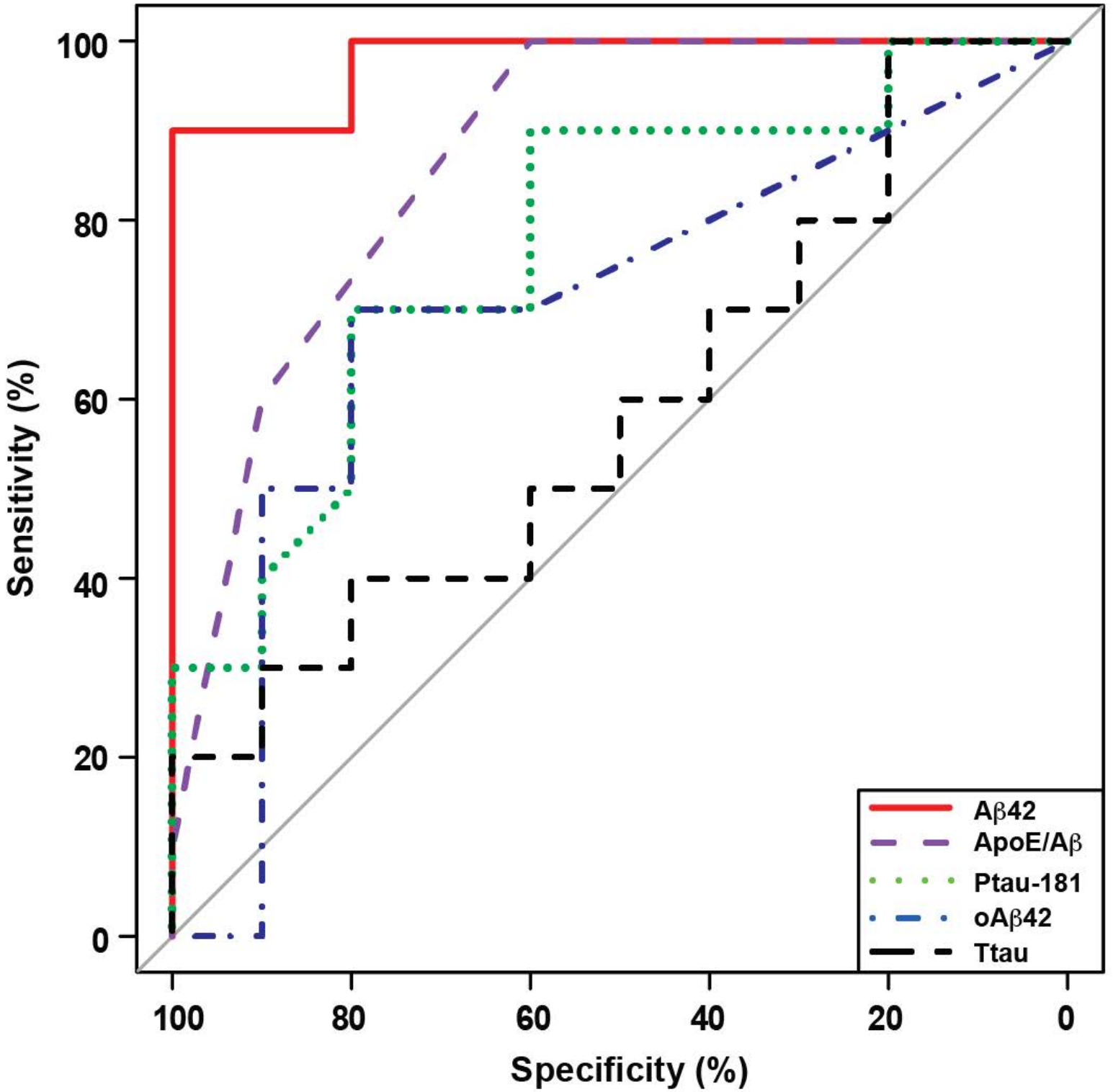

Supplementary Figure 1. Biochemical optimization of apoE/Aβ complex ELISA

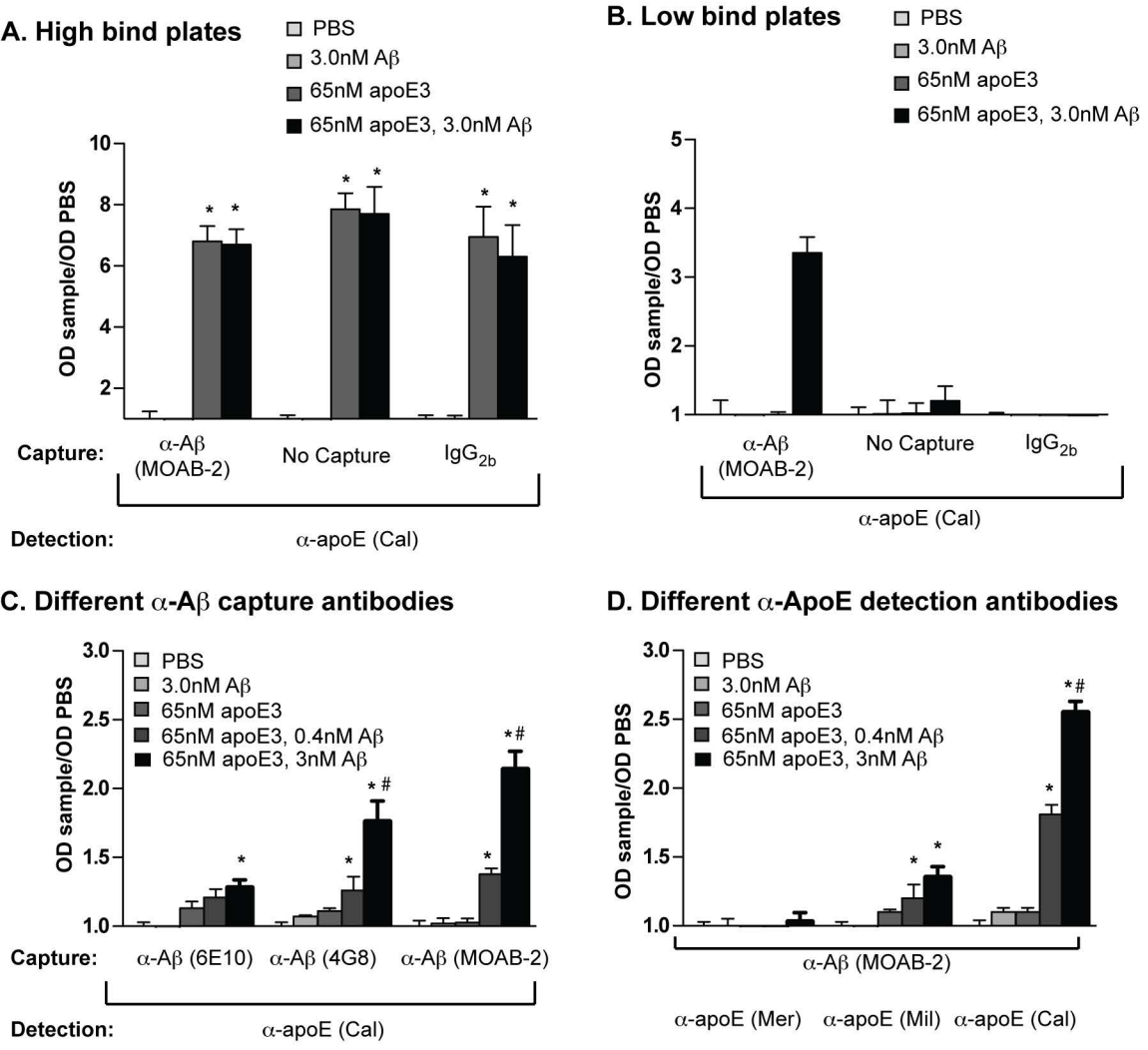

Supplementary Figure 1. Biochemical ELISA apoE/Aβ complex optimization.
ELISA detection of HEK-apoE3/Aβ complex using **(A)** High (Maxisorp™) or **(B)** Low (Microwell™) bind plates with α-Aβ (MOAB-2) capture and α-apoE (Cal) detection antibodies. ELISA detection of HEK-apoE3/Aβ complex using **(C)** different α-Aβ capture (6E10, 4G8, MOAB-2) with α-apoE (Cal) detection antibodies or **(D)** MOAB-2 capture with different α-apoE detection antibodies (α-apoE (Cal),α-apoE (Mil), α-apoE (Mer)) on low-bind plates. α-apoE antibodies from Calbiochem (Cal), Millipore (Mil) and Meridian Bioscience (Mer). α-Aβ antibodies from Covance (6E10), Senetek (4G8) and LaDu lab (MOAB-2). For all experiments n = 3 with duplicate samples. Data are expressed as mean ± SEM and were analysed by two-way ANOVA followed by Bonferroni multiple comparison post hoc analysis $*p < 0.05$, compared to a PBS control sample, $^{\#}p < 0.05$ compared to 65 nM apoE, 0.4 nM Aβ sample.

ID	Sex	Age	PMI* (h)	Diagnostic	Braak stage	*APOE* genotype
Normal cases and pathological controls						
726 [a,b]	F	97	8.5	Normal	0	3/3
789 [a,b]	F	105	9	Normal	0	3/3
A09-109 [a,b]	F	40	4	Spinacerebellar Ataxia	0	3/3
773 [a]	F	90	10	Vascular Dementia	0	3/3
7-09 [a]	F	63	6.5	Pick's Disease	0	3/3
15-09 [a,b]	M	82	14.9	Hippocampal sclerosis	4	3/3
7-11 [a]	F	105	4.25	Cognitive impairment, no dementia	3	3/3
35-10 [a]	F	108	4.35	Cognitive impairment, no dementia	3	3/3
27-10 [a,b]	F	98	4.3	Cognitive impairment, no dementia	4	3/3
36-10 [a]	M	97	6	Cognitive impairment, no dementia	4	3/3
824 [a,b]	F	86	12.5	Normal	0	3/4
758 [a]	M	93	8.5	Normal	0	3/4
735 [b]	M	82	8.5	Cognitively Normal	4	3/4
33-10 [a,b]	M	96	6.05	Cognitively Normal	4	3/4
31-09 [b]	M	71	5.15	Vascular Dementia	4	3/4
17-10 [a]	F	95	6.2	Cognitively Normal	5	3/4
12-09 [a]	M	85	6.75	Vascular Dementia	4	3/4
13-11 [a,b]	F	97	10.3	Cognitive impairment, no dementia	2	3/4
38-10 [a]	M	91	9.4	Cognitive impairment, no dementia	3	3/4
810 [b]	M	81	5	Spinacerebellar Ataxia type 2	0	4/4
Alzheimer's disease cases						
830 [b]	F	89	4.25	AD	2	3/3
788 [b]	M	82	9.5	AD (probable)	3	3/3
805 [a,b]	F	95	8.5	AD	5	3/3
10-11 [a,b]	F	90	7.25	AD	5	3/3
37-10 [a,b]	F	88	3.3	AD	5	3/3
21-10 [a,b]	F	97	6.1	AD	5	3/3
814 [a,b]	F	98	6	AD (probable)	5	3/3
A09-159 [a,b]	F	96	5	AD	6	3/3
16-11 [a,b]	F	75	6.15	AD	6	3/3
18-10 [a,b]	M	92	5.15	AD	6	3/3
39-10 [a,b]	M	90	5	AD	6	3/3
A10-05 [b]	M	82	10	AD	6	3/3
825 [b]	F	68	9.7	AD	3	3/4
737 [b]	F	76	10.8	AD (probable)	3	3/4
813 [a,b]	M	79	5.8	AD	5	3/4
718 [a]	M	83	11	AD	5	3/4
9-09 [a]	M	87	6	AD	5	3/4
745 [a]	F	92	7.5	AD	5	3/4
716 [a]	F	86	8.5	AD	6	3/4
A05-102 [a,b]	F	80	11	AD	6	3/4
10-09 [a]	F	82	4.5	AD	6	3/4
33-09 [a,b]	M	93	6.36	AD	6	3/4
13-10 [b]	F	99	4.4	AD	5	3/4
A07-163 [b]	M	82	5	AD	6	4/4
811 [b]	M	59	5.5	AD (probable)	6	4/4

Supplementary Table 1. Subject data for samples used as a source for synaptosome isolation. Human post-mortem samples were obtained from the Alzheimer's Disease Research Center Neuropathology Cores of UCLA, USC and UC Irvine**:** UC Irvine samples include samples from the 90+ study.[a] – ELISA (Fig. 3A); [b] – ELISA (Fig. 3B) [c] *PMI –post-mortem interval , AD = Alzheimer disease.

ID	Sex	Age	PMI* (h)	Diagnostic	Braak stage	*APOE* genotype
Normal cases						
1003	M	79	2.25	Normal	2	3/3
5015	M	84	2.90	Normal	1	3/3
1040	M	87	2.00	Normal	2	3/3
1142	M	92	3.25	Normal	0	3/3
5170	M	81	2.20	Normal + hemorrhage & infarcts	2	3/3
1049	F	72	3.75	Normal	1	3/3
1092	F	86	1.75	Normal	1	3/3
1103	F	76	2.00	Normal	1	3/3
1146	F	93	2.75	Normal	2	3/3
1153	F	75	3.50	Normal	1	3/3
Alzheimer's disease cases						
1016	M	83	4.00	AD	6	3/3
1037	M	82	4.00	AD + LBs in Amygdala (abundant), & Entorhinal	6	3/3
1058	M	78	3.75	AD	6	3/3
1160	M	73	2.00	AD	6	3/3
1096	M	84	4.50	AD	6	3/3
1118	F	83	3.50	AD	6	3/3
1139	F	86	2.00	AD, Late Stage	6	3/3
1215	F	91	3.00	AD (mid stage)	5	3/3
1085	F	84	5.00	AD	6	3/3
1168	F	80	4.00	AD, late stage, + micro infarct	6	3/3
1125	M	74	3.00	AD + Severe Amyloid Angiopathy	6	4/4
1173	M	75	3.75	AD + Severe amyloid angiopathy	6	4/4
1038	M	89	3.25	Mid Stage AD- Medial/Temporal Lobe Type + infarcts	5	4/4
1144	M	85	2.75	AD (mid)	6	4/4
1133	F	82	4.75	AD + Amyloid Angiopathy	6	4/4
1114	F	68	3.25	AD + Microinfarct	6	4/4
1061	F	80	2.75	AD	6	4/4
1041	F	84	3.33	AD	6	4/4
1204	F	72	2.25	AD, late stage + Limbic Lewy bodies (amygdala)	6	4/4
1109	F	77	3.00	Early AD	5	4/4

Supplementary Table 2. Subject data for samples used as a source for CSF analysis. Samples were obtained from the Alzheimer's disease center at the University of Kentucky. *PMI = Post Mortem Interval, AD = Alzheimer disease.